Multi-behavioral Multi-robot Systems driven by Motivation Dynamics

Kleio Baxevani, and Herbert G. Tanner

***Abstract*— This paper outlines a methodology for constructing multiple dynamical behaviors for a multi-agent system within the motivation dynamics theoretical framework. Recent work introduced analytical conditions for a dynamical system to undergo a Hopf bifurcation and generate multiple dynamical behaviors from a single family of continuous dynamics. The paper contributes by leveraging these recent results to develop a multi-agent system capable of switching its dynamic behavior without changing its underlying continuous dynamics. Simulation and experimental results are provided, confirming the theoretical results which guarantee the existence of a Hopf bifurcation in the dynamics of the multi-robot system.**

I. Introduction

A. Motivation

The advent of swarming and flocking control architectures based on nearest-neighbor interactions was hailed as a breakthrough a couple of decades back (e.g. [1]–[3]), giving a definitive answer to the problem of scalability of earlier, mostly centralized, multi-robot coordination architectures. For all its additional advantages in terms of robustness and simplicity of implementation, however, it appears that the paradigm merely shifted system vulnerabilities: while centralized architectures expose the central coordinator as a single point of failure, the decentralized ones that are based on nearest-neighbor interaction can still in principle be disrupted by blocking the agent interaction mechanisms.

In fact, whereas it could take a degree of sophistication for a targeted attack on the central system node to succeed and cripple the system, disrupting the interaction mechanisms in robot swarms and flocks can be relatively low tech, especially given the main argument for scalability being that the sensing and computational payload of individual group members is relatively inexpensive. Indeed, for example, image-based sensing and localization is problematic in smoke or darkness, and wireless communication can be jammed. It could be that the swarming paradigm of the early 2000's traded one type of vulnerability for another.

Ultimately, it may not be wise to completely dismiss one paradigm to fully adopt another, since both have benefits to offer, especially if a way is found to reign in scalability issues that come with the increased dimensionality. In fact, there appear to be ways to make apparently centralized multi-robot coordination architectures far more robust [4]–[6]. Interestingly, there can also be a third way: a coordination approach that neither relies on agent interaction, nor does it require the full state vector of all the robots in order to impose a desired collective behavior. This perspective highlights the distinction between the predominant Lagrangian approach to multi-agent coordination versus an arguably leaner Eulerian approach [7], taking a position closer to the latter—in the sense of a common state-dependent (but identity-independent) control vector field utilization—but without a reliance on permutation invariance properties.

The authors are with the Dept. of Mechanical Engineering, University of Delaware; Email: {kleiobax, btanner}@udel.edu.

This work is supported by NSF's SCH program via award # 2014264.

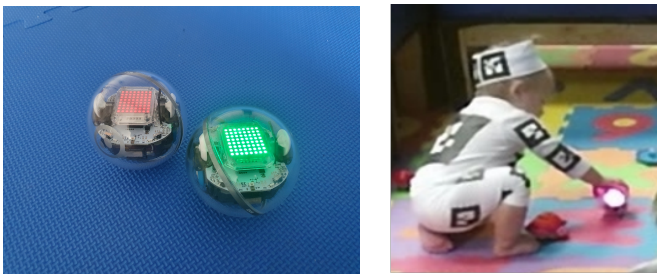

Fig. 1: (*Left*) Sphero Bolt: A commercially available educational robotic toy. (*Right*) Snapshot of infant physically interacting with Sphero [9].

In this alternative paradigm, all robots in the collective essentially receive their marching orders in the form of a common (to all) mathematical specification of desired behavior, that can be thought of as a universal feedback law broadcast by a central supervisor. There may be local reactive adjustments to this universal directive, depending on the capacity for onboard sensing, but otherwise agents do not need to interact with each other directly, and each can be acting as an individual. Interestingly from the viewpoint of robustness and resiliency, once the directive is issued and unless it is updated, there is practically nothing that can stop the swarm from executing its mission, other perhaps than the disabling of all swarm members.

There are, in fact, cases where the complete lack of inter-agent sensing and communication capabilities forces the adoption of a swarm coordination strategy in this regime. One such case is the deployment of swarms of micro robots for the delivery of biochemical payload [8]; these tiny devices have extremely limited to no capacity for sensing each other, and no potential for onboard computation and communication. Yet they can all be steered using gradient fields generated e.g., by chemicals, light, or magnets.

Another case, which is the one motivating the approach in this paper, is the utilization of collection of inexpensive, commercial-off-the-shelf (COTS) toy robots (Fig. 1) for initiating purposeful play-based social interaction between the toy system and children, in order to serve specific pediatric rehabilitation objectives [10]. In such a robot-child social interaction context, one control objective for the robot collective is to exhibit different motion behaviors depending on the children's response, to attract and preserve their

attention, focus, and active engagement. One such possibility is for the robot group to switch between periodic motion around, and convergence to, a given target (e.g., the child) in a controllable and stable manner. Here, of course, the toys themselves can be constructed to be more sophisticated from a computation and sensing standpoint, but the economic incentive for the manufacturers to do so may be lacking, and low-level system access for re-engineering can be limited.

B. Related Work

Existing work on multi-robot control with the objective of converging to a moving geometric formation around a target has been mostly based on local interaction (e.g. [11]–[13]), often using strategies that impose constant inter-agent bearing [14], [15]—extensions include the utilization of a beacon as a fixed reference [16]—in an effort to control the location of the circumcenter and the radius of the circular orbit. These control schemes, however, are inapplicable when robots cannot communicate or sense each other.

Convergence to a formation, *without* requiring local interaction can still be achieved through vector field based guidance schemes (e.g. [17]). Such schemes might not have any obstacle avoidance feature incorporated (see [18] for an exception), yet in a miniature scale, robots can recover easily from collisions usually unharmed [19], and if collisions must be avoided at all cost, then reactive schemes can still be employed if some minimal local sensing is possible [13].

Along the lines of coordinating the motion of robotic systems using reference vector fields (e.g. [20]) is an approach that allows them to switch behaviors on the fly through the adjustment of a single scalar parameter, and is based on bifurcation theory [21]. Of course, a behavior effect of this type can also be achieved in a switching or hybrid systems framework through the utilization of temporal logic (e.g. [22], [23]), but the former approach obviates several analytical (e.g. stability during switching; see [24]) and computational (e.g. model checking) considerations. In the bifurcation theory-based paradigm, the behaviors of the system are the result of the interaction between a single set of continuous navigation dynamics and a set of also continuous motivation dynamics; they can be expressed as a weighted sum with the weights taking real values in the $[0, 1]$ interval.

There is potential for bifurcation theory to be leveraged for endowing a swarm of robots with multiple collective behaviors, the latter encoded in the vector fields resulting from the nontrivial combinations of that motivational dynamics yield. At the time of this writing, there is still no instance of the utilization of this mathematical methodology for the coordination of collection of mobile robots in the peer-reviewed literature. This paper attempts to contribute into closing this gap.

C. Contribution and Paper Organization

The contribution of this paper is in outlining a new *methodology for a robot swarm to be able to exhibit multiple dynamic behaviors and rapidly switch among them, without resorting to local interaction or switching its underlying continuous dynamics*. Thus, rather than switching between a family of dynamical systems as dictated by some temporal logic protocol, the behavioral transitions are realized by updating a small finite set of constant parameters within the same swarm member dynamics.

The approach reported here follows the motivational dynamics paradigm for behavior switching. By extending earlier work in this direction that focuses on single-agent systems [25], this paper incorporates an additional meaningful tuning parameter in the agent dynamics which adjusts agent speed, and generalizes the coordination paradigm from one to many. The modification and generalization essentially allows the regulation of the intensity of the resulting vector field that steers the whole swarm, introducing an additional layer of reconfiguration and customizability to the swarm coordination protocol.

The rest of the paper is organized as follows. Section II introduces a key theorem[1] [26, Theorem 4.3.2] which establishes the conditions for the existence of a Hopf bifurcation in the multi-behavioral system of this paper. Then, Section III introduces the new parameter of the system and lays out the mathematical description of the problem considered here, and is followed by the main results of the paper in Section IV. Numerical and experimental results confirming the theoretical predictions are presented in Section V. The paper concludes by highlighting a few remarks of this work in Section VI.

II. Mathematical Preliminaries

Consider a dynamical system parameterized by a continuous constant $\mu \in \mathbb{R}$, that has $x \in \mathbb{R}^n$ as its state:

$$\dot{x} = f_\mu(x) \ , \tag{1}$$

and assume that it has an equilibrium at x_0 for $\mu = \mu_0$. For that equilibrium, suppose that the conditions of the following theorem hold (cf. [26, Theorem 3.4.2]):

Theorem 1 ([26], [27]): If the Jacobian $D_x f_{\mu_0}\big|_{x_0}$ of the right-hand-side of (1) has a simple pair of purely imaginary eigenvalues $\pm i\,\omega$ for $\omega > 0$ and no other eigenvalues with zero real parts, then there is a smooth curve of equilibria $\big(x(\mu), \mu\big)$ with $x(\mu_0) = x_0$, and the eigenvalues $\lambda(\mu), \bar{\lambda}(\mu)$ of $D_x f_{\mu_0}\big(x(\mu)\big)$ which are imaginary for $\mu = \mu_0$, vary smoothly with μ. If, in addition, $\frac{\mathrm{d}\,\mathrm{Re}\,\lambda(\mu)}{\mathrm{d}\mu}\Big|_{\mu=\mu_0} = d \neq 0$, then there exists a unique three-dimensional center manifold passing through $(x_0, \mu_0) \in \mathbb{R}^n \times \mathbb{R}$, and a smooth change of coordinates for which the Taylor expansion of (1) of degree 3 on the center manifold, is given in polar coordinates:

$$\dot{r} = (d\,\mu + a\,r^2)r \qquad \dot{\theta} = \omega + c\,\mu + b\,r^2 \ ,$$

for suitable constants a, b, and c. For $a \neq 0$, there is a surface of periodic solutions on the center manifold, and

- if $a > 0$, the periodic solutions are repelling; whereas
- if $a < 0$, the periodic solutions are stable limit cycles.

$\diamond$

[1]The theorem statement is slightly adapted here for simplicity and completeness, suppressing some background information which is not central to this analysis.

In view of Theorem 1, let $w = (x, y) \in \mathcal{D} \subseteq \mathbb{R}^2$, and consider planar *component vector fields* $F_i(w) : \mathcal{D} \to T\mathcal{D}$, for $i \in \{1, 2\}$. Each vector field has an *associated (Lyapunov) function* $f_i : \mathcal{D} \to \mathbb{R}$ for which it is known that

$$\dot{f}_i = \nabla^\intercal f_i \, F_i \leq 0 \ ,$$

with equality when evaluated at the equilibrium points.

Now let m_1, and m_2 represent scalar variables ranging in the interval $[0, 1]$, such that $m_1 + m_2 = \rho$, where $\rho \in \mathbb{R}^+$ is a tunable regulation parameter. Then, one can define the *motivation state* of the system as the pair (m_1, m_2), with each m_i having its own dynamics.

Based on F_i and m_i, the *navigation dynamics* is defined as a new dynamical system formed as a convex combination of F_i using the motivation state variables m_i as weights

$$\dot{w} \triangleq m_1(t) \cdot F_1(w) + m_2(t) \cdot F_2(w) \ . \tag{2}$$

Intuitively, each m_i expresses the degree to which the dynamical behavior captured by F_i manifests itself in (2).

Define now the *mean-difference* coordinates

$$\bar{F} \triangleq \frac{F_1(w) + F_2(w)}{2} \qquad \Delta F \triangleq F_1(w) - F_2(w) \tag{3a}$$

$$\bar{f} \triangleq \frac{f_1(w) + f_2(w)}{2} \qquad \Delta f \triangleq f_1(w) - f_2(w) \tag{3b}$$

$$\bar{m} \triangleq \frac{m_1(t) + m_2(t)}{2} \qquad \Delta m \triangleq m_1(t) - m_2(t) \ , \tag{3c}$$

in terms of which, (2) can be expressed as

$$\dot{w} = \tfrac{1}{2}(\Delta m \cdot \Delta F + 4\bar{m} \cdot \bar{F}) \ . \tag{4}$$

Now fix $\bar{m} = \rho/2$, and for $\sigma \in \mathbb{R}$ impose the following dynamics on Δm:

$$\frac{\mathrm{d}\Delta m}{\mathrm{d}t} = \Delta m \, (\sigma - \Delta m^2) + \Delta f \, (1 - \Delta m^2) \ , \tag{5}$$

which will be referred to as the *motivation dynamics* of the combined system. The motivation dynamics introduce a pitchfork Hopf bifurcation with σ as its parameter [28].

Having fixed $\bar{m}$, (4) now reduces to

$$\dot{w} = \tfrac{1}{2}\Delta m \cdot \Delta F + \rho \, \bar{F} \ . \tag{6}$$

Definition 1: An equilibrium $(w_d, \Delta m_d)$ of (5)–(6) is called a *deadlock* if $\Delta m_d = 0$. ◇

III. Problem Formulation

A. Problem statement

Consider a collection of N robots moving on the plane, each located at $(x_{r_j}, y_{r_j}, \theta_{r_j})$ and having unicycle dynamics of the form

$$\dot{x}_{r_j} = v_j \cos\theta_{r_j} \qquad \dot{y}_{r_j} = v_j \sin\theta_{r_j} \qquad \dot{\theta}_{r_j} = \omega_j \ , \tag{7}$$

for $j = \{1, \ldots, N\}$ and assume that each has an output defined as

$$\eta_j = h_j(x_{r_j}, y_{r_j}) = \begin{bmatrix} x_{r_j} + \varepsilon\cos\theta_{r_j} \\ y_{r_j} + \varepsilon\sin\theta_{r_j} \end{bmatrix} \ , \tag{8}$$

for some small $\varepsilon > 0$. It is well known that this system is output feedback linearizable (see e.g. [29]), so the input transformation will not be repeated here.

The control objective for this robot collection is to follow a reference vector field, appropriately defined through (2), which will steer them along four different attractors, namely three distinct planar limit cycles and a stable node, selecting on-line the desired attractor through the choice of a finite set of parameters.

For $i \in \mathbb{N}$, and for $(x_{ci}, y_{ci}) \in \mathbb{R}^2$, $r_i > 0$, consider planar vector fields F_i of the form:

$$\dot{x} = r_i(y - y_{ci})$$

$$\dot{y} = -r_i(x - x_{ci})\big[(x - x_{ci})^2 + (y - y_{ci})^2 - r_i^2\big] \tag{9a}$$

$$\quad - (y - y_{ci})\big[(x - x_{ci})^2 + (y - y_{ci})^2 - r_i^2\big] \ . \tag{9b}$$

These vector fields admit stable limit cycles that have the shape of circles centered at (x_{ci}, y_{ci}) with radii r_i. The associated Lyapunov functions for the vector fields in (9) is given in the generic form

$$f_i(x, y) = \tfrac{1}{2}\big[(x - x_{ci})^2 + (y - y_{ci})^2 - r_i^2\big]^2 \ .$$

The control objective is to design navigation and motivation dynamics (5)–(6) that can exhibit a *multitude* of stable steady-state behaviors, including those expressed by (9) but also distinct others, depending on the choice of μ.

B. Assumptions

For the purposes of the analysis in this paper, the following simplifying assumptions are made:

Assumption 1: $i \in \{1, 2\}$.

Assumption 2: $r_i = r > 0$.

The following assumption simplifies analysis without any significant loss of generality:

Assumption 3:

$$(x_{c1}, y_{c1}) = (0, 0) \ , \qquad y_{c2} = 0 \ , \qquad x_{c2} = x_{\mathrm{dis}} > 0 \ .$$

With these assumptions in place, the expressions for the component vector fields and their associated Lyapunov functions reduce to

$$F_1 : \begin{cases} \dot{x} = ry - x(x^2 + y^2 - r^2) \\ \dot{y} = -rx - y(x^2 + y^2 - r^2) \end{cases} \tag{10a}$$

$$F_2 : \begin{cases} \dot{x} = ry - (x - x_{\mathrm{dis}})[(x - x_{\mathrm{dis}})^2 + y^2 - r^2] \\ \dot{y} = -r(x - x_{\mathrm{dis}}) - y[(x - x_{\mathrm{dis}})^2 + y^2 - r^2] \end{cases} \tag{10b}$$

and

$$f_1(x, y) = \frac{(x^2 + y^2 - r^2)^2}{2} \tag{11a}$$

$$f_2(x, y) = \frac{[(x - x_{\mathrm{dis}})^2 + y^2 - r^2]^2}{2} \ . \tag{11b}$$

IV. Main Results

Proposition 1 (cf. [25]): Given (10)–(11), there is a deadlock for (5)–(6) at $(w_d, \Delta m_d) = (x_{\mathrm{dis}}/2, 0, 0)$. ◇

Proof: A detailed proof of Proposition 1 for the specific case where $\rho = 1$ can be found in [25]. The proof of Proposition 1, follows closely on the footsteps of that of the related result in [25], and thus only a sketch is outlined below.

With Definition 1 allowing $\Delta m_d = 0$, one has

$$\left.\frac{\mathrm{d}\Delta m}{\mathrm{d}t}\right|_{\Delta m_d = 0} = 0 \overset{(5)}{\Longrightarrow} \Delta f = 0$$

$$\overset{(3b)(11)}{\Longrightarrow} f_1(w_d) = f_2(w_d) \ . \tag{12}$$

One of the solutions of (12) is $x_d = {}^{x_{\rm dis}}/_2$. Substituting into (6)—given that $(w_d, \Delta m_d)$ is equilibrium (and recalling that $w = (x, y)$)—yields

$$\frac{\mathrm{d}x}{\mathrm{d}t}\Big|_{x_d,\Delta m_d} = 0 \overset{(6)}{\Longrightarrow} \rho \bar{F}_x\,|_{x_d,\Delta m_d} = 0 \overset{(3a)(10)}{\Longrightarrow} y_d = 0 \ ,$$

which suggests that $y_d = 0$. Therefore, the equilibrium coordinates are indeed $(w_d, \Delta m_d) = ({}^{x_{\rm dis}}/_2, 0, 0)$. ■

The Jacobian of the system vector field (5)–(6) is a 3-dimensional matrix represented in the form

$$J(w, \Delta m) = \begin{bmatrix} J_{11} & J_{12} & J_{13} \\ J_{21} & J_{22} & J_{23} \\ J_{31} & J_{32} & J_{33} \end{bmatrix} \ , \tag{13}$$

which is naturally parameterized by $x_{\rm dis}$, r, ρ, and σ, given (10) and (5). Matrix $J(w, \Delta m)$ evaluated at the deadlock, yields: $J_d \triangleq J(w, \Delta m)\,|_{w=w_d, \Delta m = \Delta m_d}$.

Proposition 2 (cf. [25]): Under the following two conditions on the elements of $J_d \triangleq J(w, \Delta m)\,|_{w=w_d,\Delta m=\Delta m_d}$:

(i) The equality constraint:

$$\begin{aligned} &- J_{11}^2(J_{22}+J_{33}) - J_{22}^2(J_{11}+J_{33}) - J_{33}^2(J_{22}+J_{33}) \\ &+ J_{11}J_{12}J_{21} + J_{11}J_{13}J_{31} + J_{22}J_{23}J_{32} \\ &+ J_{22}J_{12}J_{21} + J_{33}J_{23}J_{32} + J_{33}J_{13}J_{31} + \\ &J_{12}J_{23}J_{31} + J_{21}J_{13}J_{32} - 2J_{11}J_{22}J_{33} = 0 \ , \end{aligned} \tag{14a}$$

(ii) and the inequality constraint (tr denotes trace):

$$\mathrm{tr}\, J_d = J_{11} + J_{22} + J_{33} < 0 \ , \tag{14b}$$

the Jacobian of system (5)–(6) evaluated at the deadlock has two purely imaginary, and one negative real eigenvalue. ◇

Proof: The detailed proof of Proposition 2 for the case of $\rho = 1$ can be found in [25]. The general case is not included in this paper since the same steps can be followed without the inclusion of ρ to disturb the argumentation. ■

The trace of the Jacobian seen in (14b) can be written as a function of $(r, x_{\rm dis}, \rho, \sigma)$:

$$\mathrm{tr} J_d = \sigma + 0.5\rho\left(2r^2 - 0.5x_{\rm dis}^2\right) + 0.5\rho\left(2r^2 - 1.5x_{\rm dis}^2\right) \ .$$

Defining

$$\begin{aligned} P(r, x_{\rm dis}, \rho) \triangleq\ & r^8 x_{\rm dis}^4 - r^6 x_{\rm dis}^6 + a_1\rho^2 r^6 x_{\rm dis}^4 + a_2\rho^2 r^6 x_{\rm dis}^2 \\ &+ a_3\rho^4 r^6 + a_4 r^4 x_{\rm dis}^8 - a_1\rho\, r^4 x_{\rm dis}^6 + (\rho^4 - 6\rho^2) r^4 x_{\rm dis}^4 \\ &+ (\rho^2 - \rho^4) r^2 x_{\rm dis}^6 - a_3\rho^4 r^4 x_{\rm dis}^2 + a_5\, r^2 x_{\rm dis}^{10} - a_5\rho^2\, r^2 x_{\rm dis}^8 \\ &+ a_6\rho^4 r^2 x_{\rm dis}^4 + a_7\, x_{\rm dis}^{12} + a_5\rho^2\, x_{\rm dis}^{10} + a_8\rho^4\, x_{\rm dis}^8 \ , \end{aligned} \tag{15}$$

with coefficients $a_1 = 2$, $a_2 = 8$, $a_3 = -16$, $a_4 = 0.375$, $a_5 = -0.0625$, $a_6 = -4$, $a_7 = 0.00390625$, and $a_8 = 0.25$, and identifying condition (14a) of Proposition 2 as a 2nd order polynomial in σ, allows one to express the two possible solutions for σ in terms of $x_{\rm dis}, r$ as follows:

$$\begin{aligned} \sigma_{1,2} = \frac{1}{2\rho\left(2r^2 - x_{\rm dis}^2\right)}\Big[&- (x_{\rm dis}^2 + 4\rho^2) r^4 \\ &+ (0.5x_{\rm dis}^2 + 4\rho^2 r^2) x_{\rm dis}^2 r^2 \\ &- 0.0625\, x_{\rm dis}^6 - \rho^2 x_{\rm dis}^4 \pm \sqrt{P(r, x_{\rm dis})}\Big] \ . \end{aligned} \tag{16}$$

In the case of $P(r, x_{\rm dis}) < 0$, both solutions drawn by (16) are complex and are discarded; then it is acknowledged that there no Hopf bifurcation that can be triggered for the particular choice of $(x_{\rm dis}, r, \rho)$. For a real solution for σ, and to guarantee the existence of a Hopf bifurcation, the second condition (14b) should also be satisfied. Hence, there exists a choice of $(x_{\rm dis}, r, \rho)$ for which the corresponding bifurcation parameter solution given by (14a), also satisfies:

$$\sigma < \rho\, x_{\rm dis}^2 - 2\rho\, r^2 \ . \tag{17}$$

Ultimately, a real solution of (16) which also satisfies (17) signifies the existence of a Hopf bifurcation; in fact, it becomes itself the critical value for the bifurcation parameter which is henceforth referred to simply as σ.

V. Validation

A. Simulation Results

Consider two limit cycles generated by (10) with radius $r = 1.2$ and distance between the two centers $x_{\rm dis} = 2.5$ with the associated Lyapunov functions given by (11) as shown in Fig. 2a, and the regulation parameter of the system is set at $\rho = 0.75$. Proposition 1, indicates that a deadlock of the system where $\bar{F} = 0$ and $\Delta f = 0$ exists at $w_d = (1.25, 0)$.

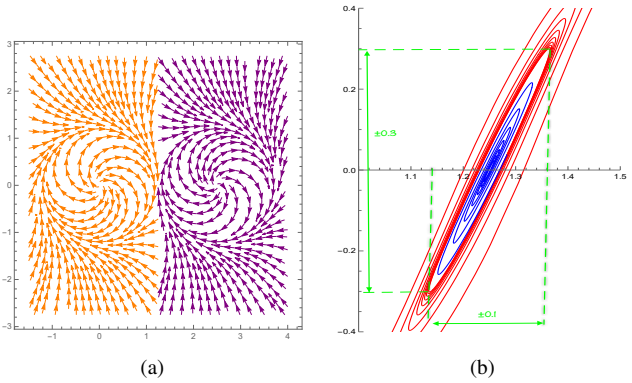

(a) (b)

Fig. 2: (a) Component vector fields F_1 and F_2 as limit cycles of radii $r = 1.2$ and with centers $x_{dis} = 2.5$ apart. (b) Flow lines of the navigation dynamics with $\sigma = 0.4 > \sigma_c$, (red) converging to an elliptical limit cycle, and with $\sigma = 0.3 > \sigma_c$ (blue) converging to the deadlock.

Equation (16) suggests that critical value of the bifurcation parameter for a system with parameters $(x_{\rm dis}, r, \rho) = (2.5, 1.2, 0.75)$, is $\sigma_c = 0.362$. As it can be verified, this critical value of the bifurcation parameter satisfies both conditions of Theorem 1 since the Jacobian (13) has two purely imaginary eigenvalues and one negative real eigenvalue:

$$\lambda_{1,2} = \pm 0.46\, i \ , \qquad \lambda_3 = -2.16 \ ,$$

while

$$\frac{\mathrm{d}\lambda}{\mathrm{d}\sigma}\Big|_{\sigma=0.362} = 0.051 \neq 0 \ .$$

Figure 2b shows the paths of a robotic agent driven by the motivational dynamics with two different instantiations of the bifurcation parameter. When $\sigma = 0.4 > \sigma_c$, the agent undergoes an eliptical limit cycle; when the bifurcation parameter is reset to $\sigma = 0.3 < \sigma_c$, the limit cycle disappears and the agent is led to converge to the deadlock.

The behavior of a robotic agent driven by all the features of the navigation-motivation dynamics of (6)–(5) is illustrated in Fig. 3. First, the motivational dynamics are frozen $\dot{w} = \frac{\mathrm{d}\Delta m}{\mathrm{d}t} = 0$ at values $m_1 = 0.75$ and $m_2 = 0$ for 100 seconds, letting the component vector field F_1 fully express itself; then the motivational dynamics variables are reset to $m_1 = 0$ and $m_2 = 0.75$, allowing the component vector field F_2 fully express itself instead for another 100 seconds; following that, the motivational dynamics are let to evolve with $\sigma = 0.4 > \sigma_c$ in the 200–300 second interval, triggering a limit cycle in between F_1 and F_2; and finally, in the 300–400 second interval, the bifurcation parameter is reset to $\sigma = 0.3 < \sigma_c$, forcing the agent to converge to the deadlock located at $(1.25, 0)$. It is noteworthy that all four behaviors are produced by the same vector field structure given by (2) (or (6), equivalently), with different settings of the driving motivational dynamics (5).

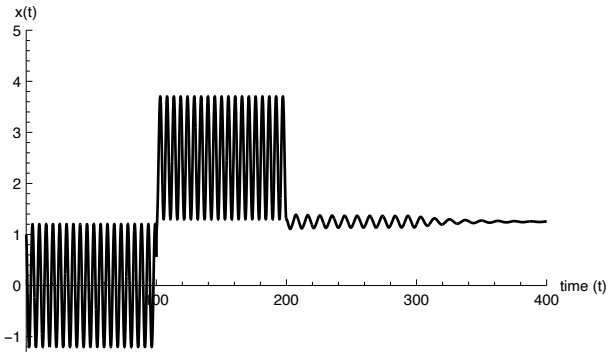

Fig. 3: The x coordinate of an agent continuously undergoing all behavior regimes encoded in the motivational dynamics: first the circular limit cycle centered at $(0, 0)$ and radius 1.2 in the time interval $[0, 100]$; then the circular limit cycle centered at $(2.5, 0)$ with the same radius for the interval $[100, 200]$; then the elliptical limit cycle around the deadlock at $(1.25, 0)$ for $t \in [200, 300]$; and finally the convergence to the deadlock over the interval $[300, 400]$.

Figure 4 illustrates the composite behavior of a group of five agents as it is reflected in the full state dynamics $(x, y, \Delta m)$, i.e., the agents' planar position, as well as the state of the motivational dynamics regulating the composite reference vector field that drives them. The figure makes it clearer that as the time-invariant component vector fields are blended with the help of the motivational dynamics, the resulting reference vector field is now time-varying. The system starts evolving with the bifurcation parameter set above the critical value $\sigma = 0.4 > \sigma_c$. In this case the reference vector field steers them all into the elliptical limit cycle, on which they stably converge and follow for 80 seconds. At $t_c = 80\,\mathrm{s}$ the bifurcation parameter resets instantaneously to a value less than the critical, $\sigma' = 0.3 < \sigma_c$. Consequently, the behavior of the system switches, and the agents' states continuously transition to a new behavior where they converge to the deadlock at $(1.25, 0)$.

B. Experimental Results

The objective of this preliminary experimental trial is to validate the implementability of the vector field approach to multiple physical robots sharing the same workspace and directed by the same navigational dynamics. While the group

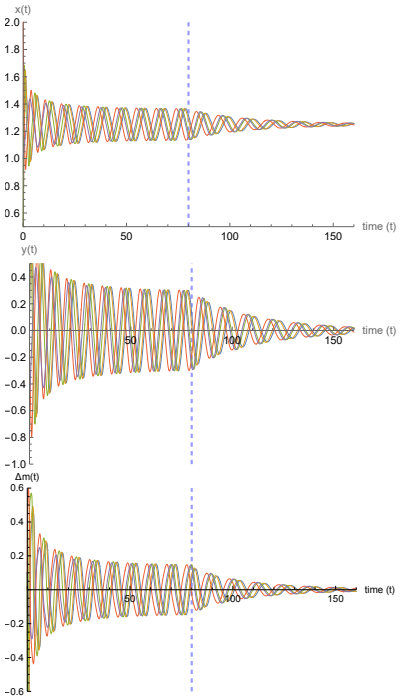

Fig. 4: The system is simulated starting with the bifurcation parameter set at $\sigma = 0.4$ admitting a limit cycle. At time $t_c = 80$ sec the bifurcation parameter changes to $\sigma = 0.3$ (blue dashed line), and the system switches to the converging behavior in a continuous manner.

size in this first trial is minimal ($n = 2$), it still is indicative of at least two things: (i) physical robots that cannot directly communicate and are unaware of each other's presence can still be coordinated through some shared navigational dynamics, and that (ii) experimental observations match simulation results in terms of the ability of the robots exhibit different behaviors using the *same* motivational dynamics but with a different value of the bifurcation parameter each time. Both robots move at the same desired constant speed of 20 cm/s.

The navigation dynamics utilized in this experimental trial are exactly the one created in simulation, with parameters set as $(x^2_{\mathrm{dis}} = 2.5, r = 1.2, \rho = 0.75)$. The two robotic agents were realized in the form of Sphero Bolt robots (Fig. 1-*Left*). The robots are equipped with an LED array, which a Zed overhead camera uses to localize them through color detection, and are directed to track the navigational dynamics reference vector field. Figure 5 shows the estimated x and y planar coordinates of the two robots when they follow the field with $\sigma = 0.3 < \sigma_c$, and $\sigma = 0.4 > \sigma_c$. The measurements are admittedly noisy, not only due to the color detection scheme but primarily due to the incapability of these toy robots to precisely position themselves, in addition to them moving on a bumpy foamy surface (Fig. 1-*Left*) where they will be interacting with children. The physical volume also needs to be factored in when assessing their motion in Fig. 5a, as it is impossible for both robots to occupy the same exact location in space. Similarly, when moving along the elliptical limit cycle created when the bifurcation parameter crosses the critical threshold in Fig. 5b, the closed curve's eccentricity often forces them to collide producing

additional motion disturbances. Still, the periodicity of the steady state behavior is still visible in Fig. 5b and the range of oscillation matches the shape and size of the limit cycle (Fig. 2a).

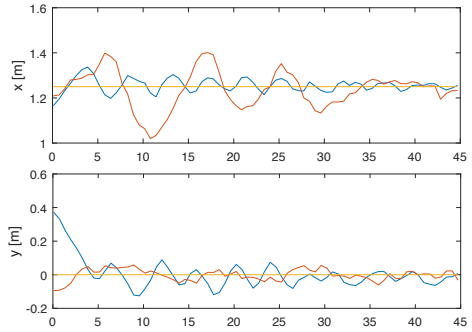

(a) Convergence to deadlock for $\sigma = 0.3$

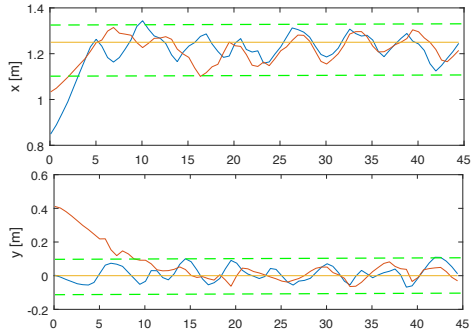

(b) Convergence to limit cycle for $\sigma = 0.4$

Fig. 5: Behavior of two spheros steered by the navigational dynamics to converge to a point (a), and to a limit cycle (b) using the same motivational dynamics with different bifurcation parameters. The horizontal axis in all graphs measures time in seconds.

VI. Conclusion

Swarms of robots that can neither sense nor communicate can still be coordinated to exhibit multiple dynamical behaviors using navigational dynamics, tunable through a small set of parameters, as a reference velocity field common to all swarm members. One of the parameters determines the nature of the swarm member's trajectories, while the other regulates the desired speed along the path. This paper demonstrates the potential of this type of tunable navigational dynamics to coordinate groups of minimally instrumented robots through a common feedback control law that does not rely on robot-to-robot interaction.

References

[1] H. G. Tanner, A. Jadbabaie, and G. J. Pappas, "Stable flocking of mobile agents, part I: Fixed topology," in *Proceedings of the IEEE Conference on Decision and Control*, 2003, pp. 2010–2015.

[2] ——, "Stable flocking of mobile agents, part II: Dynamic topology," in *Proceedings of the IEEE Conference on Decision and Control*, 2003, pp. 2016–2021.

[3] R. O. Saber, "Flocking for multi-agent dynamic systems: algorithms and theory," *IEEE Transactions on Automatic Control*, vol. 51, no. 3, pp. 401–420, 2007.

[4] K. Baxevani, A. Zehfroosh, and H. G. Tanner, "Resilient supervisory multi-agent systems," *IEEE Transactions on Robotics*, vol. 38, no. 1, pp. 229–243, 2022.

[5] X. Yu, D. Shishika, D. Saldana, and M. A. Hsieh, "Modular robot formation and routing for resilient consensus," in *Proceedings of the American Control Conference*, 2020, pp. 2464–2471.

[6] K. Saulnier, D. Saldana, A. Prorok, G. J. Pappas, and V. Kumar, "Resilient flocking for mobile robot teams," *IEEE Robotics and Automation Letters*, vol. 2, no. 2, pp. 1039–1046, 2017.

[7] P. Kingston and M. Egerstedt, "Index-free multi-agent systems: An eulerian approach," *IFAC Proceedings Volumes*, vol. 43, no. 19, pp. 215–220, 2010.

[8] S. Das, E. E. Hunter, N. A. DeLateur, E. B. Steager, R. Weiss, and V. Kumar, "Cellular expression through morphogen delivery by light activated magnetic microrobots," *Journal of Micro-Bio Robotics*, vol. 15, no. 2, pp. 79–90, 2019.

[9] G. R. Kouvoutsakis, K. Baxevani, H. G. Tanner, and E. Kokkoni, "Feasibility of using the robot sphero to promote perceptual-motor exploration in infants," in *Proceedings of the 2022 ACM/IEEE International Conference on Human-Robot Interaction*, 2022, pp. 850–854.

[10] A. Zehfroosh and H. G. Tanner, "Reactive motion planning for temporal logic tasks without workspace discretization," *In Proceedings of the IEEE American Control Conference*, 2019.

[11] H. Tanner and D. Christodoulakis, "Cooperation between aerial and ground vehicle groups for reconnaissance missions," in *Proceedings of the IEEE Conference on Decision and Control*, 2006, pp. 5918–5923.

[12] L. A. Valbuena Reyes and H. G. Tanner, "Flocking, formation control, and path following for a group of mobile robots," *IEEE Transactions on Control Systems Technology*, vol. 23, no. 4, pp. 1268–1282, 2015.

[13] I. Yadav and H. G. Tanner, "Mobile radiation source interception by aerial robot swarms," in *Proceedings of the 2nd IEEE International Symposium on Multi-Robot and Multi-Agent Systems*, 2019, pp. 63–69.

[14] J. A. Marshall, M. E. Broucke, and B. A. Francis, "Formations of vehicles in cyclic pursuit," *IEEE Transactions on Automatic Control*, vol. 49, no. 11, pp. 1963–1974, 2004.

[15] U. Halder, B. Schlotfeldt, and P. Krishnaprasad, "Steering for beacon pursuit under limited sensing," in *Proceedings of the IEEE 55th Conference on Decision and Control*, 2016, pp. 3848–3855.

[16] K. S. Galloway and B. Dey, "Collective motion under beacon-referenced cyclic pursuit," *Automatica*, vol. 91, pp. 17–26, 2018.

[17] H. G. Tanner, S. Loizou, and K. J. Kyriakopoulos, "Nonholonomic navigation and control of cooperating mobile manipulators," *IEEE Transactions on Robotics and Automation*, vol. 19, no. 1, pp. 53–64, 2003.

[18] H. G. Tanner and A. Boddu, "Multi-agent navigation functions revisited," *IEEE Transactions on Robotics*, vol. 28, no. 6, pp. 1346–1359, 2012.

[19] A. Stager and H. Tanner, "Composition of local potential functions with reflection," in *Proceedings of the IEEE International Conference on Robotics and Automation*, 2019, pp. 5558–5564.

[20] D. Panagou, H. G. Tanner, and K. J. Kyriakopoulos, "Nonholonomic control design via reference vector fields and output regulation," *ASME Journal of Dynamic Systems, Measurement and Control*, vol. 137, no. 8, pp. 2831–2836, 2015.

[21] P. B. Reverdy and D. E. Koditschek, "A dynamical system for prioritizing and coordinating motivations," *SIAM Journal of Applied Dynamical Systems*, vol. 17, pp. 1683–1715, 2018.

[22] J. Liu and N. Ozay, "Abstraction, discretization, and robustness in temporal logic control of dynamical systems," in *Proceedings of the 17th International Conference on Hybrid Systems: Computation and Control*, 2014, p. 293–302.

[23] S. Coogan, E. A. Gol, M. Arcak, and C. Belta, "Traffic network control from temporal logic specifications," *IEEE Transactions on Control of Network Systems*, vol. 3, no. 2, pp. 162–172, 2016.

[24] L. R. Valbuena and H. G. Tanner, "Hybrid potential field based control of differential drive mobile robots," *Journal of Intelligent & Robotic Systems*, vol. 68, pp. 307–322, 2012.

[25] K. Baxevani and H. G. Tanner, "Constructing continuous multi-behavioral planar systems through motivation dynamics and bifurcations," in *Proceedings of the IEEE Conference on Decision and Control*, 2021, pp. 1095–1100.

[26] J. Guckenheimer and P. Holmes, *Nonlinear Oscilations, Dynamical Systems, and Bifurcation of Vector Fields*. Springer-Verlag, 1983.

[27] F. Verduzco, "The first Lyapunov coefficient for a class of systems," in *Triennial IFAC World Congress*, 2005, pp. 1205–1209.

[28] P. B. Reverdy, "A route to limit cycles via unfolding the pitchfork with feedback," in *Proceedings of the American Control Conference*, 2019, pp. 3057–3062.

[29] L. R. Valbuena and H. G. Tanner, "Flocking, formation control and path following for a group of mobile robots," *IEEE Transactions on Control Systems Technology*, vol. 23, no. 4, pp. 1268–1282, 2015.